Integrated geophysical interpretation for groundwater potentiality at Wadi Ghubba, Central Sinai, Egypt

H. M. Mekhemer
Water Resources Research Institute (WRRI)[1]

S. A. Sultan, M. A. Abd Alla
National Research Institute of Astronomy and Geophysics[2]

L. Brimich
Geophysical Institute of the Slovak Academy of Sciences[3]

F. M. Santos
Physics Department and CGUL[4]

A b s t r a c t : Groundwater in Sinai is the main objective for different developing programs. It can be prospected by exploring new aquifers containing water of appreciable amounts and good quality. To outline the expected aquifers, different geophysical tools were used in the study area. These geophysical tools are geoelectric, magnetic, and gravity methods. Fifteen deep vertical electrical soundings have been measured with current electrode spacing ranges between AB = 10 m and AB = 6000 m to define the main aquifers in the studied area.

All vertical electrical sounding measurements (VES) were re-interpreted by using IPI-1D program. The actual thicknesses and resistivities were used to construct geoelectrical cross-section to define subsurface stratigraphic units and water bearing aquifer. The geoelectrical cross-section shows that the subsurface section consists of five geoelectric units. The first unit is limestone overlying clay unit. The third unit is limestone, while the fourth unit is clayey limestone. The last unit is Nubian sandstone of Lower Cretaceous deposits which forms the main aquifer. The depth of the upper surface of the Nubian sandstone (aquifer) ranges between 334 to 980 m. One hundred and fifty land magnetic stations were measured to cover the studied area. The interpretation of the magnetic

[1] National Water Research Center (NWRC), Egypt; e-mail: m_hatem_m_@yahoo.com, h.mekhemer@wrri.org.eg
[2] Helwan, 11722 Cairo, Egypt; e-mail: tarakhan66@hotmail.com
[3] Dúbravská cesta 9, 845 28 Bratislava, Slovak Republic; e-mail: geofbrim@savba.sk
[4] University of Lisbon, Lisbon, Portugal

data started with reduction to the magnetic pole, then depth to the upper surface of the basement was determined applying the Eulier deconvolution technique. The results of magnetic interpretation show that the depth of the basement surface ranges between 1270 m at the northwestern corner and 2720 m at the southern part of the study area. Gravity measurements were taken using Autograv gravimeter of sensitivity 0.01 mGal at the same stations of magnetic measurements. Regional-residual separation was carried out using high and low pass filter technique. The residual gravity anomaly map was used to detect the structural elements. There are normal faults whose directions are: NW-SE, N-S and NE-SW.

Key words: aquifer, water, geoelectric methods gravimetry, magnetic methods, VES

1. Introduction

The area of study was occupied by small temporary settlements. The main activity is the grazing on temporary grasses growing during rainy season. In order to develop permanent settlements, the construction of dominant water resources new promising aquifers have to be explored. In order to achieve this target the integrated geophysical tools are used for groundwater exploration, especially geoelectric, gravity and magnetic methods. The geoelectric tool was used for detecting and differentiating between the subsurface layers. Quantitative interpretation of the vertical electrical sounding curves was done by using the two layer standard curves and generalized Cagniard graphs *(Koefoed, 1960; Orellana and Money, 1966)* to determine the thickness and true resistivities for each geoelectrical unit in order to obtain a preliminary model. Gravity method is a successful tool for detecting the trends of the structural elements after applying the filter. Magnetic method is very important to detect the upper surface of the basement. Different authors used the integrated geophysical interpretation for groundwater exploration as *Hassanen et al. (2001)* who used geoelectric, gravity and magnetic tools for groundwater exploration at Nukhil area, central Sinai. *Sultan and Sorady (2001)* used the tools of geoelectrical and gravity for detecting the structural elements and groundwater exploration at northwestern part of Sinai. Also, *Santos et al. (2006)* used the joint inverse for the geoelectrical and gravity data for groundwater exploration

at northwestern part of Sinai.

The study area lies around wadi Al Ghubba north Egma plateau of central part of Sinai and located at latitudes $29°28'$ and $30°03'$ longitudes $33°07'$ and $33°50'$ as shown in Fig. 1. The surface geology of the study area is described by the geological map of Sinai 1:500 000 shown in Fig. 2 executed by *UNSECO Cairo Office (2005)*. Most of the study area was covered by Pleistocene and Paleocene deposits. Pleistocene deposits are composed of alluvium deposits, while Paleocene deposits, the so called Esena shale formation, is composed of marly shale. The eastern part of the study area is covered by Lower Eocene and Upper Cretaceous rock units. The Lower Eocene is represented by Egma Formation of chalky limestone. The Upper Cretaceous was represented by Sudr, Duwi, Matulla and Wata formations. Sudr Formation is mainly chalk of Maastrichtian age. Duwai formation is

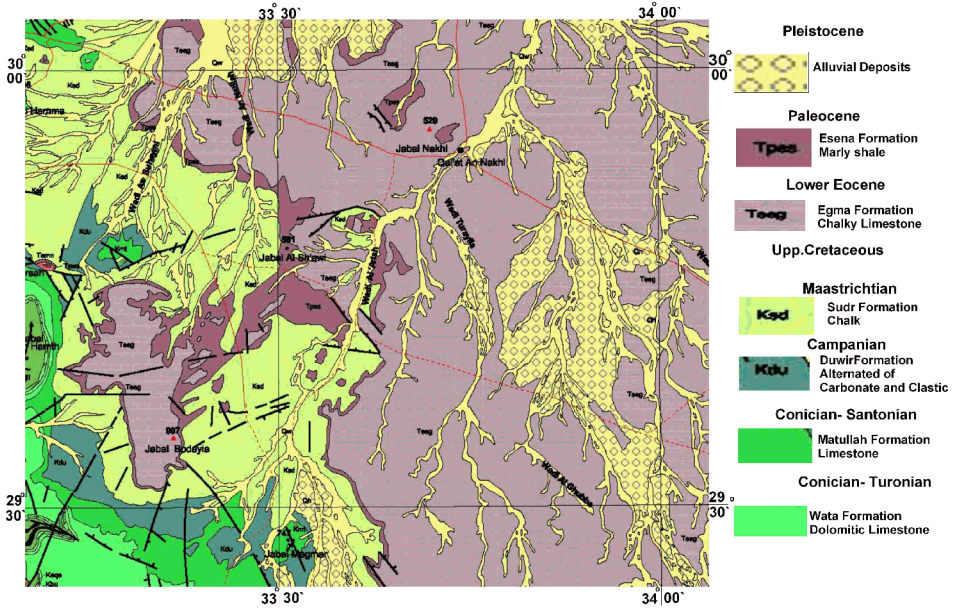Fig. 1. Location map of the study area.

389

Fig. 2. Geological map of the study area after UNSECO, 2005.

composed of alternated carbonate and clastic of Campanian age. Matullah formation is composed of limestone of Conician-Santonian age. Wata formation is composed of dolomitic limestone of Conician-Turonian age.

2. Measurements of geophysical data and interpretation

2.1. Geoelectrical data

The geoelectrical data that were measured in the study area by vertical electrical soundings by Shlumberger configuration is considered the best array for groundwater exploration. Fifteen vertical electrical soundings were measured to cover the study area with AB/2 ranges from 5 to 3000 m. This large configuration is needed to penetrate more depths to detect the Nubian sandstone, which is the main aquifer in the study area. Fig. 3 shows the

location of geophysical measurements by using CH-8708A transmitter and EPR0121A recorder instruments. Two VES were measured at and near two bore-holes. At the bore-holes (JICA-1), VES 13 was measured and VES 10 measured near bore-hole (JICA-3). The results of the two bore-holes utilized for the correlation and calibration of the VES curve parameters (layer resistivity and thickness) of the interpreted electrical data with the geologic information (lithology and thickness) are shown in Table 1 and the table attached to Fig. 4.
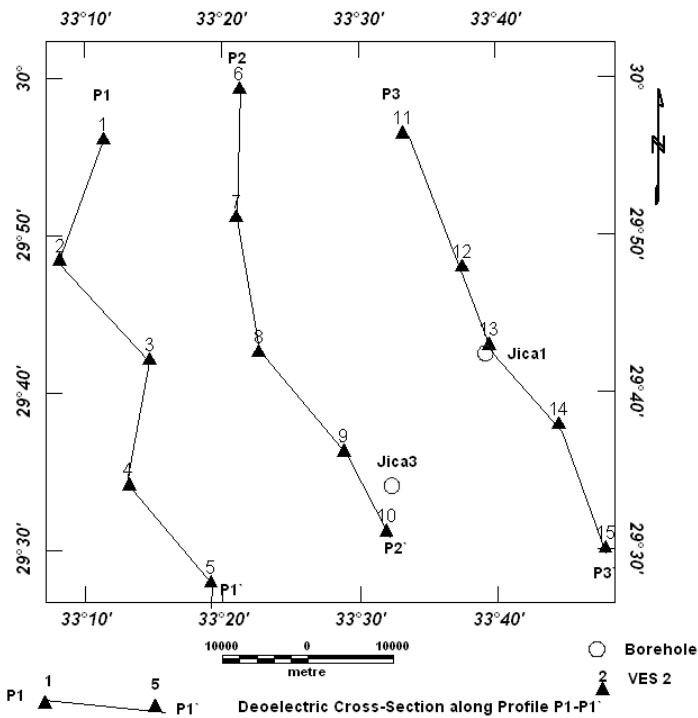

Fig. 3. Location map of the geophysical measurements.

Quantitative interpretation technique was applied to determine the thicknesses and true resistivities of the successive layers below each VES station using the measured field curves. The authors used a method of manual (graphical) interpretation, which depends on using two layer standard curves and generalized Cagniard graphs *(Koefoed, 1960)* to delineate from the VES

Table 1. Results of Bore-Hole (JICA 1)

Depth (m)		Age	Description
From	To		
0	50	Paleocene	Wadi Deposits
50	180	Maastrichtian	Limestone intercalated with clay
180	270	Campanian	Claystone
270	385	Santonian-Coniacian	Limestone intercalated with clay
385	450	Turonian	Limestone
450	520		Chalky Limestone
520	585	Cenomanian	Limestone intercalated with clay
585	640		Limestone
640	670		Limestone intercalated with clay
670	700		Limestone
700	770		Limestone intercalated with clay
770	810		Limestone
810	865		Limestone intercalated with clay
810	1115	Lower Cretaceous	Alternation of shale and Sandstone
1115	1260	Jurassic	Sand and Shale

curve a number of geoelectric layers having corresponding values of thickness and true resistivity. The results of manual interpretation are used as initial models for IBI2WIN software to compute the true depths and resistivities for each VES curve. The results of interpretation of these vertical electrical soundings revealed the existence of four major resistivity layers with true resistivity values ranging between 2 and 412 Ohm.m and thickness ranged between 1.4 and 462 m as shown in Fig. 4.

Three geoelectric cross-sections were constructed along the profiles shown in Figs. 5 through 7 by plotting the true resistivities and the interpreted layer thicknesses as vertical columns. These geoelectric cross-sections are compared with gravity profiles to determine the locations of the interpreted faults. The interpretation of the geoelectric cross-sections indicates that the shallow subsurface lithologic sequence of the study area is made up of four geoelectric zones of relative resistivities as ($\rho_1 < \rho_2 > \rho_3 < \rho_4$). The first geoelectric zone is characterized by very low resistivity values ranging from 5 to 70 Ohm.m and having thickness varying from 80 to 276 m which correlate with clay. The second geoelectric zone shows relatively

high resistivity values ranging from 6 to 145 Ohm.m and thickness ranging from 26 to 404 m corresponding to limestone. The third geoelectric unit is characterized by relatively low resistivity values. Lithologically, this zone consists of limestone intercalated with clay and contains saline and brackish water. The fourth layer is characterized by relatively high resistivity values ranging from 64 to 412 Ohm.m and corresponding to sand and sandstone. This layer is the main groundwater aquifer in the study area and contains fresh water according to the results of bore holes.

2.2. Gravity data

The gravity measurements were taken using CG-3 Autograv (automatic gravity meter) made by Scintrex with resolution of 0.01 mGal. Hundred and fifty gravity stations were selected to cover the study area. Different corrections were deduced, using specialized *Geosoft Program (1998)* such as drift, tide, latitude, free-air and Bouguer corrections. Also, terrain correction was carried out, using Bible chart to estimate the elevation points of different zones and execute terrain correction through the Geosoft program.

The corrected gravity values were plotted and contoured in map and processed to represent Bouguer anomaly map of contour interval 1 mGal, as shown in Fig. 8. The interpretation of the Bouguer anomaly map starts with separating the anomalies related to shallow depths (residual anomalies)
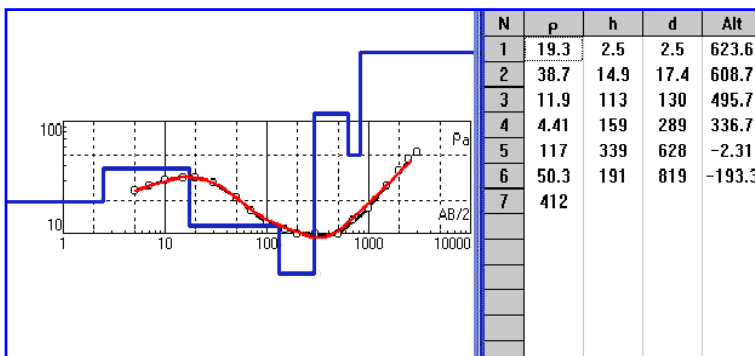

N	ρ	h	d	Alt
1	19.3	2.5	2.5	623.6
2	38.7	14.9	17.4	608.7
3	11.9	113	130	495.7
4	4.41	159	289	336.7
5	117	339	628	−2.31
6	50.3	191	819	−193.3
7	412			

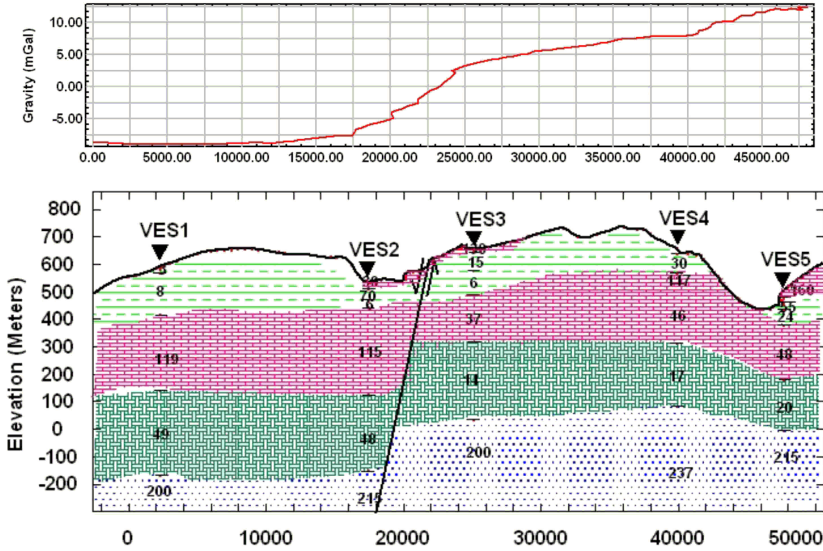Fig. 4. Interpretation of VES 13 using IPI2W.

Fig. 5. Geoelectric cross-section along Profile P1 compared with gravity profile.
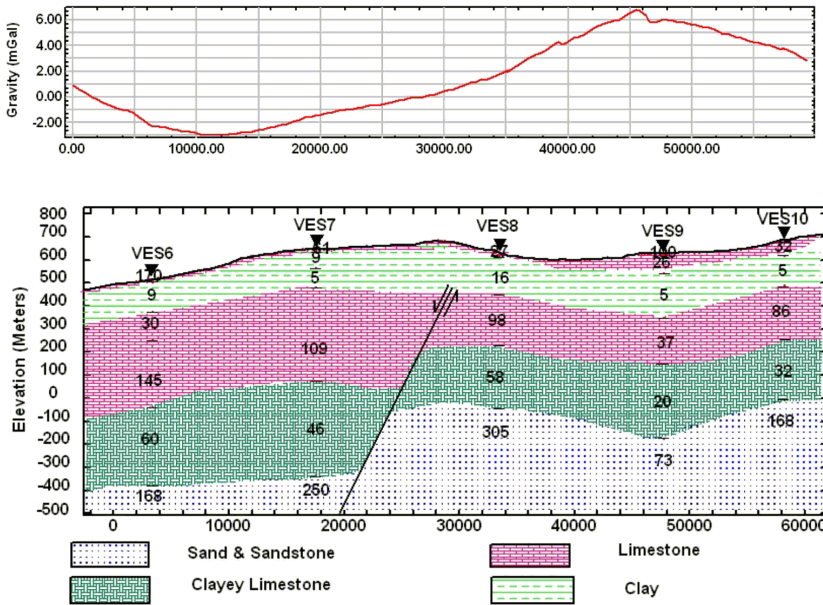

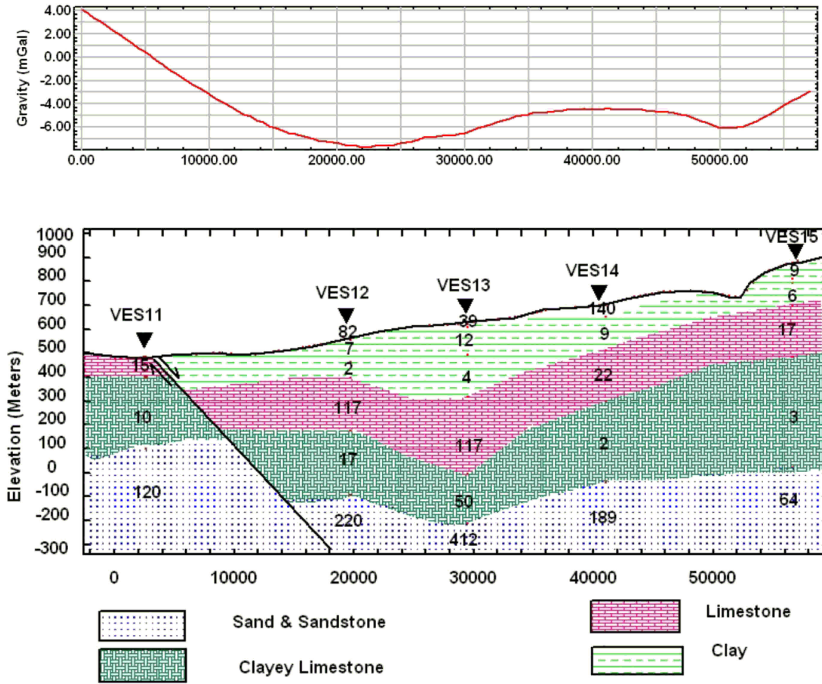Fig. 6. Geoelectric cross-section along Profile P2 compared with gravity profile.

Fig. 7. Geoelectric cross-section along Profile P3 compared with gravity profile.

from those of deeper sources (regional anomalies). The authors used high-pass and low pass filter technique to separate the two components. The separation was carried out at wave number 0.0002 (1/km). Fig. 9 shows the regional Bouguer anomaly map, which indicates that the deep-seated sources are deeper at the southeastern part and become shallower towards southwest. Fig. 10 shows the residual Bouguer anomaly map which indicates different trends of the structural elements such as NE-SW, NW-SE and N-S trends.

2.3. Magnetic data

The total intensity magnetic field measurements are carried out with the Envimag magnetometer (model Scintrex) made in Canada of one nT sensitivity at the same places of gravity stations. The values of the magnetic

stations are corrected for diurnal variations and normal gradient of earth magnetic field (IGRF). After correcting the magnetic values, the corrected data are stored in the computer to carry out the gridding and contouring processes by *Geosoft programs (Oasis Montaj), 1998* to produce the total intensity magnetic map Fig. 11. The interpretation of the magnetic data starts by converting the data of total intensity to reduce to magnetic pole Fig. 12, where the magnetic fields created by geological bodies are distorted by the inclination and declination of the earth's field. This can be attributed to the fact that at low or moderate angles of inclination of the geomagnetic field, the peaks of the anomalies have to be shifted away from over the centers of the magnetized bodies, making it difficult to determine correctly the shapes and locations of these magnetized bodies. To overcome this distortion in the appearance of an anomaly, its magnetic latitude and the corresponding variations of the dip angle of the magnetization vector in the body have to be considered. A mathematical procedure is adopted on a grid of values of the contour map of the total magnetic intensity. This mathematical procedure was first described by *Baranov (1957, 1975;*
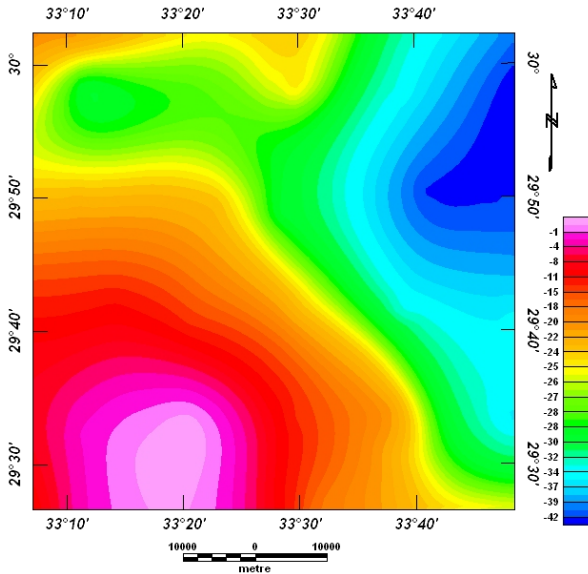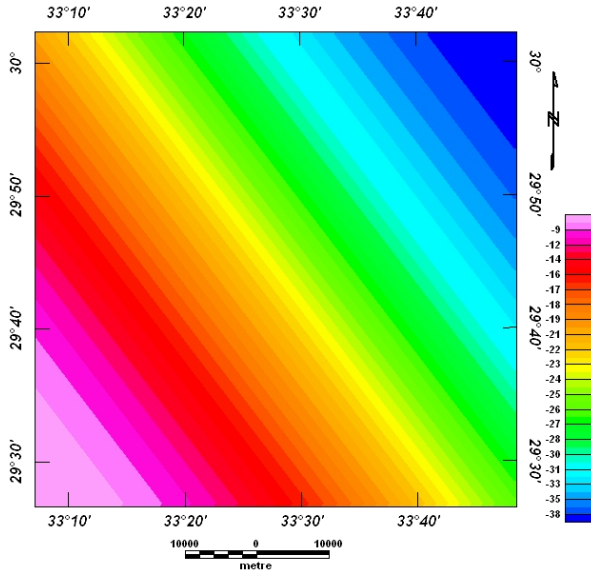
Fig. 8. Bouguer anomaly map.
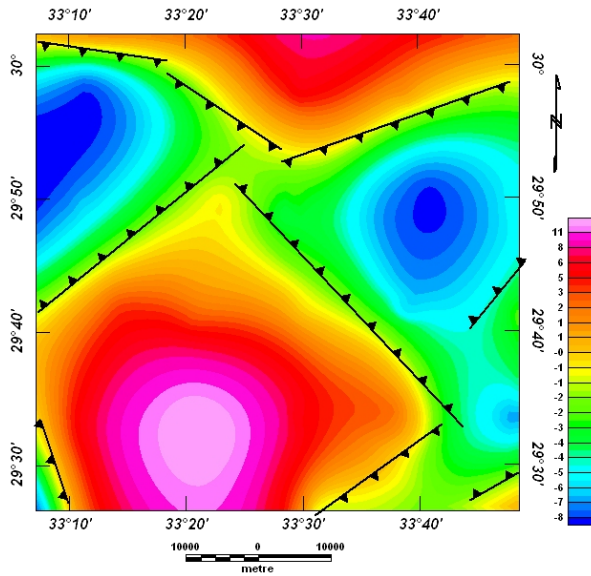
Fig. 9. Regional Bouguer anomaly map.

Fig. 10. Residual Bouguer anomaly map.

Bhattacharya, 1968). In the present study, the total intensity magnetic map reduced to the pole can be calculated automatically by using Geosoft program.

The principal application of magnetic data is to determine the depth to the top of the geologic sources that produce observed anomalies. The depth estimation is often used to determine the depth and location of geologic units or structures that produce a magnetic anomaly. Moreover, the quantitative interpretation of the total intensity magnetic map is carried out by using GRIDEPTH program, which is the one of *Geosoft programs package (1998)*. GRIDEPTH program is an automatic location and depth determination method for gridded magnetic based upon Euler's homogeneity equation. However, the Euler's homogeneity equation relates the field (magnetic) and its gradient components to the location of the source, with the degree of homogeneity N, which may be interpreted as a structural index *(Thompson, 1982)*. The structural index is a measure of the rate of change of a field with distance, for example, a magnetic field narrow 2-D dyke has a structural index of N = 1, while a vertical pipe gives N = 2 and Magnetic step and contact gives N = 0. We used structural index = 0, since the step and contact are dominant in the study area.

The essential benefit of the magnetic interpretation is its use for geological mapping of basement surface, where the magnetic surveying provides basic information about the nature and configuration of the crystalline. The results of magnetic depth determination using Euler's deconvolution shown in Fig. 13 indicate that the shallow depths of the basement are located at the northwestern part of the study area 1270 m, while the deepest depths are located at the southern and central part of the study area up to 2720 meters.

3. Discussion

The results of integrated geophysical interpretation for the different geoelectrical, gravity, and magnetic methods gave good results by comparing it with boreholes data and the geological setting of the study area. The interpretation of geoelectrical data indicate that there are four layers, the first one is similar to the result of the borehole data which consists of clay
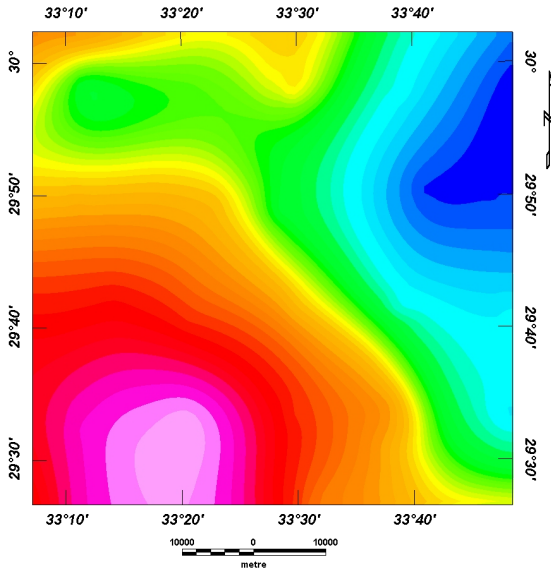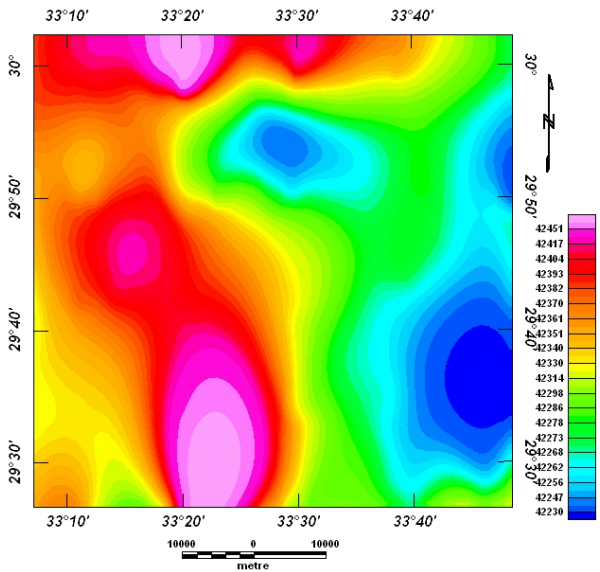
Fig. 11. Total intensity magnetic map.

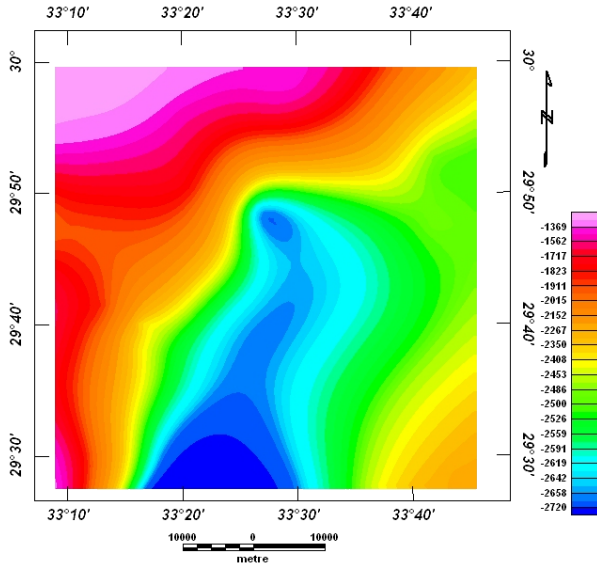Fig. 12. Total intensity magnetic map reduced to the pole.

399

Fig. 13. Depth to the basement surface map.

and have low resistivity values. The second layer is characterized by high resistivity values and similar to the limestone of borehole. The third one is composed of limestone intercalated with shale which decreases the resistivity values. The fourth layer is characterized by high resistivity values, and compared to the sand and sandy clay and sandstone. The structural element from the gravity interpretation shows also the main direction for the gulf of Aquba and Gulf of Suez and Nile valley trends.

4. Conclusion

From the results of the interpretation for the geoelectrical, gravity, and magnetic data, it can be concluded that:

1. The subsurface section of the study area consists of four geoelectrical units, which are clay, limestone, clayey limestone and sandstone.
2. The main aquifer in the study area is the fourth layer and consists of sand and sandstone and contains good quality fresh water.

400

3. The area is affected by different fault elements of NW-SE, NE-SW and N-S trends.

4. The depth of the basement rocks ranges between 1270 and 2720 m.

References

Baranov V., 1957: A new method for interpretation of aeromagnetic maps; pseudo-gravimeric anomalies. Geophys., **22**, 2, 359–383.

Baranov V., 1975: Potential field data and their transformation in applied geophysics geoexploration. Monographs, series 1-6, Gebuuder Borntaeger, Berlin-Stuttgart, Germany.

Bhattacharya P. K., 1968: Continuous spectrum of the total magnetic field anomaly due to a rectangular prismatic body. Geophys., **31**, 97–121.

Geosoft Programs, 1998: Geosoft mapping and processing system. Geosoft Inc., Suit 500, Richmond St. West Toronto, ON, Canada N5UIV6.

Hassanen A. Gh., Sultan S. A., Mohamed B. S., 2001: Integrated geophysical interpretation for groundwater exploration at Nukhl Area, Central Sinai. Bull. of National Res. Insit. of Astronomy & Geophysics, Ser. B, 2001, 283–298.

IPI2Win-1D Program, 2000: Programs set for 1-D VES data interpretation. Dept. of Geophysics, Geological Faculty, Moscow University, Russia.

Koefoed O., 1960: A generalized Cagniard graph for interpretation of geoelectric sounding data. Geophysical Prospecting, **8**, 3, 459–469.

Orellana E., Money H. M., 1966: Master tables and curves for vertical electrical soundings over layered structure. Madras, Ciecia, 150 p.

Santos F. A. M., Sultan S. A., Patricia R., El Sorady A. L., 2006: Joint inversion of gravity and geoelectrical data for groundwater and structural investigation: application to the northwestern part of Sinai, Egypt. Geophys. J. Int., **165**, 705–718.

Sultan S. A., El Sorady A. L., 2001: Geoelectric and gravity measurements for groundwater exploration and detection of structural elements at Romana area, Northwest of Sinai, Egypt. In: Proceedings of the 6th Conf. Geology of Sinai for Development, Ismailia, 109–120.

Thompson D. T. T., 1982: Euler, a new technique for making computer assisted depth estimates from magnetic data. Geophys., **47**, 31–37.

UNSECO Cairo Office, 2005: Geologic Map of Sinai, Egypt, Scale 1:500 000. Project for the Capacity Building of the Egyptian Geological survey and Mining Authority and the National Authority for Remote Sensing and Space Sciences in Cooperation with UNDP and UNSECO, Geological Survey of Egypt.

WRRI & JICA, 1999: South Sinai Groundwater Resources Study in the Arab Republic
of Egypt.